

The Hsa_circ_0091579/miR-940/TACR1 Axis Regulates the Development of Hepatocellular Carcinoma

This article was published in the following Dove Press journal:
Cancer Management and Research

Peiqiang Jiang
Wei Han
Yu Fu
Qingmin Chen

Department of Hepatobiliary and
Pancreatic Surgery, The First Hospital of
Jilin University, Changchun, Jilin, People's
Republic of China

Purpose: Circular RNAs (circRNAs) play important roles in hepatocellular carcinoma (HCC) development. The circRNA *hsa_circ_0091579* (*circ_0091579*) is dysregulated in HCC, while the mechanism of *circ_0091579* in HCC development is largely unknown.

Patients and Methods: Thirty paired cancer and adjacent normal tissues were harvested from HCC patients. SNU-387 and Huh7 cells were cultured in this study. *circ_0091579*, *microRNA-940* (*miR-940*) and *tachykinin-1 receptor* (*TACR1*) abundances were measured via quantitative reverse transcription-polymerase chain reaction or Western blot. Cell viability, migration, invasion, colony ability, cell cycle distribution and apoptosis were assessed via 3-(4,5-dimethyl-2-thiazolyl)-2,5-diphenyltetrazolium bromide, transwell assay, colony formation assay and flow cytometry. The interaction among *circ_0091579*, *miR-940* and *TACR1* was tested via dual-luciferase reporter analysis. The anti-HCC role of *circ_0091579* knockdown in vivo was investigated using xenograft model.

Results: *circ_0091579* expression was enhanced in HCC tissue samples and cells. *circ_0091579* silence inhibited cell viability, migration, invasion and colony formation, induced cell cycle arrest at G0/G1 phase, and promoted apoptosis in HCC cells. *miR-940* was increased via *circ_0091579* and *miR-940* knockdown reversed the suppressive effect of *circ_0091579* silence on HCC development. *miR-940* targeted *TACR1* to repress HCC development. *circ_0091579* could regulate *TACR1* expression by mediating *miR-940*. Down-regulation of *circ_0091579* decreased xenograft tumor growth.

Conclusion: Knockdown of *circ_0091579* repressed HCC development by mediating *miR-940/TACR1* axis, indicating a new pathogenesis of HCC.

Keywords: hepatocellular carcinoma, *hsa_circ_0091579*, *miR-940*, *TACR1*

Introduction

Hepatocellular carcinoma (HCC) accounts for up to 90% of liver malignancy with high incidence and mortality in the world.¹ With significant insight into the pathogenesis of HCC, the diagnosis and treatment of HCC have gained great advance.^{2,3} Nevertheless, the outcome and effective therapy strategies are poor in HCC at advanced stage. Therefore, it is urgent to explore new target for HCC treatment.

Circular RNAs (circRNAs) are a type of highly expressed RNAs formed by a closed-loop structure without the 5' caps and 3' tail, which play important roles in human cancers.⁴ CircRNAs have multi-functions in the pathogenesis, development and treatment of HCC.⁵ Moreover, circRNAs usually take part in the development and treatment of HCC by mediating the competing endogenous RNA (ceRNA)

Correspondence: Qingmin Chen
Department of Hepatobiliary and
Pancreatic Surgery, The First Hospital of
Jilin University, No. 71 Xinmin Street,
Changchun, Jilin 130021, People's Republic
of China
Tel +86-431-81875133
Email chenqingminchqm@163.com

network (circRNA-microRNA (miRNA)-mRNA).⁶ Previous studies have provided insight into multiple circRNAs in HCC. For example, *hsa_circ_0001955*, *hsa_circ_0056836* and *hsa_circ_0000092* have been reported to facilitate HCC development,⁷⁻⁹ while some circRNAs play the tumor-suppressive role in HCC, such as *hsa_circ_5692*, *hsa_circ_0070269* and *hsa_circ_0003418*.¹⁰⁻¹² A previous study reports that *hsa_circ_0091579* (*circ_0091579*), a dysregulated circRNA derived from *glypican 3* (*GPC3*) gene, is implicated in the detection, prognosis and treatment of HCC.¹³ However, the mechanism that *circ_0091579* participates in the regulation of HCC development remains largely unknown.

miRNAs are single-stranded RNAs (~20 nucleotides) which exhibit important clinical values in liver disorders, including HCC.^{14,15} The former evidences indicate that *miR-940* could play an anti-cancer role in HCC via inhibiting cell growth, migration and invasion.^{16,17} The *tachykinin-1 receptor* (*TACR1*) has been suggested to be an oncogene in many malignancies, including HCC.¹⁸⁻²⁰ The bioinformatics analysis using CircInteractome²¹ and TargatScan²² predicts that *miR-940* could bind with *circ_0091579* and *TACR1*. However, it is not clear whether *miR-940* and *TACR1* are associated with *circ_0091579*-mediated HCC development.

In this research, we detected the expression of *circ_0091579* and investigated the function of *circ_0091579* on HCC development in vivo and in vitro. Additionally, we explored the ceRNA network of *circ_0091579/miR-940/TACR1* in HCC cells.

Patients and Methods

Patients and Tissues

HCC patients (n=30) were recruited from the First Hospital of Jilin University. The HCC tissues and adjacent normal tissues were harvested and maintained at -80°C. Patients did not receive the other therapy before the tissue collection. All patients signed the written informed consents, and they provided the approval that the tissues could be stored and used for research. This work was in accordance with the Declaration of Helsinki. This research was approved via the ethics committee of the First Hospital of Jilin University.

Cell Culture and Transfection

HCC cell lines SNU-387 and Huh7 cells, and liver epithelial cell line THLE-2 cells were provided via Procell

(Wuhan, China) and grown in RPMI-1640 medium (Procell) plus 10% fetal bovine serum (Zhejiang Tianhang Biotechnology, Huzhou, China) and 1% penicillin/streptomycin (Thermo Fisher, Waltham, MA, USA) in 5% CO₂ at 37°C.

TACR1 overexpression vector (pc-TACR1) was generated by cloning *TACR1* sequence into pcDNA3.1 vector in our laboratory, and the pcDNA3.1 vector (Thermo Fisher) acted as negative control (pc-NC). siRNA for *circ_0091579* (si-*circ_0091579*-1, 5'-GCACAUU AAC CAGAGGCCUUU-3'; si-*circ_0091579*-2, 5'-CAUUAAC CAGAGGCCUUUGAA-3'), negative control of siRNA (si-NC, 5'-AAGACAUUGUGUCUCCGCCTT-3'), *miR-940* mimic (5'-AAGCAAGGGCCCGCCUCCCC-3'), negative control of mimic (miR-NC, 5'-ACGUGACACGUAUCCGACGATT-3'), *miR-940* inhibitor (5'-GGGGAGCCGGGCCCCGCCU-3'), and negative control of inhibitor (inhibitor-NC, 5'-CAGUACUUUUGUGUAGUACAA-3') were generated via Ribobio (Guangzhou, China). The vectors or these oligonucleotides (30 μM) were transfected into SNU-387 and Huh7 cells via Lipofectamin 2000 (Thermo Fisher) for 24 h.

Quantitative Reverse Transcription Polymerase Chain Reaction (qRT-PCR)

Tissues or cells were incubated in Trizol reagent (Thermo Fisher) and then total RNA was extracted using the acid guanidinium thiocyanate-phenol-chloroform extraction method.²³ The reverse transcription was conducted using the specific reverse transcription kit (Thermo Fisher), and the generated cDNA was mixed with SYBR (Solarbio, Beijing, China) and specific primers (Genscript, Nanjing, China), followed via qRT-PCR. The primers were shown as: *circ_0091579* (sense, 5'-TGAGCCAGTGGTCAGTCAAA-3'; antisense, 5'-GTGGAGTCAGGCTTGGGTAG-3'), *GPC3* (sense, 5'-CCATGCCAAGA ACTACACCA-3'; antisense, 5'-GCCCTTCATTTTCAGCTCAT-3'), *miR-940* (sense, 5'-GTATAAAGGGCCCCCGCT-3'; antisense, 5'-AGGGTCCGAGGTATTCGCACT-3'), *U6* (sense, 5'-CTCGCTTCGGCAGCACA-3'; antisense, AACGCTTCACGAATTTGCGT), and *GAPDH* (sense, 5'-TGAATGGGCAGCCGTTAGG-3'; antisense, 5'-TGGACTCCACGACGTACTCA-3'). *U6* or *GAPDH* acted as reference control. Relative expression of *circ_0091579*, *GPC3* or *miR-940* was calculated via the 2^{-ΔΔCt} method.²⁴

RNase R Treatment and Structure of *circ_0091579*

RNase R could digest the linear RNAs but not the circRNAs. To test the stability of circRNAs, the isolated RNA was incubated with 3 U/ μ g RNase R (Genesee, Guangzhou, China) for 30 min. Then, the levels of *circ_0091579* and *GPC3* were detected via qRT-PCR.

Furthermore, the structure of *circ_0091579* was explored via the cancer-specific circRNA database (<http://gb.whu.edu.cn/CSCD>).²⁵

Cell Viability

Cell viability was examined via 3-(4,5-dimethyl-2-thiazolyl)-2,5-diphenyl-2-H-tetrazolium bromide (MTT) analysis. 1×10^4 SNU-387 and Huh7 cells were added into 96-well plates and incubated for 48 h. Next, the MTT solution (Solarbio) was placed into each well with a final concentration of 0.5 mg/mL, and cells were cultured for 4 h. Then, the medium was removed and 100 μ L of dimethyl sulfoxide (DMSO; Beyotime, Shanghai, China) was added. The absorbance at 570 nm was determined with a microplate reader (Molecular Devices, Sunnyvale, CA, USA). Cell viability was normalized to the control group.

Transwell Analysis

Transwell analysis was carried out to analyze the abilities of cell migration and invasion. For invasion assay, the transwell chamber (BD, Franklin Lakes, NJ, USA) was coated with Matrigel (BD). With regard to migration analysis, the chamber was not coated with Matrigel. 1×10^5 SNU-387 and Huh7 cells in non-serum medium were placed in the top chambers. The lower chambers were added with 600 μ L of medium plus 10% serum. The cells were cultured for 20 h, and then cells passed the membranes were stained with 0.5% crystal violet (Beyotime), and counted under a microscope (Nikon, Tokyo, Japan) with 3 random fields.

Colony Formation Assay

For colony formation assay, 500 SNU-387 and Huh7 cells were added into the 6-well plates. After culture for 10 days, the cells were fixed with methanol (Aladdin, Shanghai, China) and stained with 0.5% crystal violet. The colonies were observed and counted.

Flow Cytometry

Cell cycle distribution and apoptosis were measured via flow cytometry. For cell cycle detection, 2×10^5 SNU-387 and

Huh7 cells were maintained in 6-well plates for 48 h, and then fixed with 75% ethanol (Aladdin), followed by incubating with 50 μ g/mL propidium iodide (PI; Solarbio) and RNase (Thermo Fisher). The cell cycle distribution was tested using a flow cytometer (Agilent, Hangzhou, China).

For cell apoptosis assay, 2×10^5 SNU-387 and Huh7 cells were placed into 6-well plates and incubated for 48 h. Then, the cells were harvested and incubated with Annexin V-FITC binding buffer (Sigma, St. Louis, MO, USA), followed via dyeing with Annexin V-FITC (Sigma) and propidium iodide (PI). Next, they were detected with a flow cytometer. The apoptosis rate was presented as the percentage of cells with Annexin V-FITC⁺ and PI[±].

Western Blot

Protein samples were extracted using RIPA buffer (Solarbio) and quantified using a BCA kit (Abcam, Cambridge, MA, USA). Twenty μ g protein samples were separated via sodium dodecyl sulfate-polyacrylamide gel electrophoresis and transferred to nitrocellulose membranes (Solarbio). The transferred membranes were blocked in 5% fat-free milk, and then interacted with primary antibody anti-TACR1 (ab131091, 1:1000 dilution) or anti-GAPDH (ab9485, 1:5000 dilution), which were provided via Abcam. Then, the membranes were interacted with horseradish peroxidase-conjugated IgG (ab205718, 1:20000 dilution, Abcam). GAPDH served as a loading reference. Next, the membranes were incubated with ECL reagent (Beyotime). The protein blots were tested via Image Pro Plus software (Media Cybernetics, Rockville, MD, USA).

Dual-Luciferase Reporter Analysis

The complementary sequence of *circ_0091579* and *miR-940* was searched by CircInteractome,²¹ and the sequence of *miR-940* and *TACR1* was analyzed by TargetScan.²² The wild-type luciferase reporter plasmids (WT-*circ_0091579* and WT-*TACR1*-3'UTR) were constructed by cloning the wild-type sequence of *circ_0091579* or *TACR1* 3'UTR into pGL3-control vectors (YouBio, Changsha, China). The mutant-type luciferase reporter plasmids (MUT-*circ_0091579* and MUT-*TACR1*-3'UTR) were generated via mutating the corresponding binding sites of *miR-940*. SNU-387 and Huh7 cells were co-transfected with these constructed vectors, Renilla luciferase vector, and *miR-940* mimic or miRNA NC for 24 h. Next, the luciferase activity was examined via a dual-luciferase analysis kit (Genomeditech, Shanghai, China).

Xenograft Model

The lentiviral vector carrying shRNA for *circ_0091579* (sh-*circ_0091579*) and its negative control (sh-NC) were produced via GenePharma (Shanghai, China), and transfected into Huh7 cells. The stably transfected cells were selected. Twelve BALB/c nude mice (male, 5-week-old) were purchased from Shanghai SLAC Laboratory Animal Co., Ltd. (Shanghai, China) and arbitrarily grouped into sh-*circ_0091579* or sh-NC group (n=6/group) after the corresponding subcutaneous inoculation of the transfected Huh7 cells (4×10^6 cells/mouse). The tumor size was examined once a week and calculated with the formula: $0.5 \times \text{length} \times \text{width}^2$. Twenty-eight days after inoculation, mice were killed, and all xenograft tumors were collected for weight and detection of *circ_0091579*, *miR-940* and *TACR1* expression. The animal experiments were performed in line with guidelines of the National Institutes of Health guide for the Care and Use of Laboratory animals (NIH Publications No. 8023, revised 1978), and had procured the permission of the Animal Ethical Committee of the First Hospital of Jilin University.

Statistical Analysis

The experiments were conducted 3 times. The data were shown as mean \pm SD. The difference was tested via Student's *t*-test or ANOVA with Dunnett's test using SPSS 19.0 (SPSS, Chicago, IL, USA). It was statistically significant when $P < 0.05$.

Results

circ_0091579 Level is Increased in HCC

We first measured the abnormally expressed *circ_0091579* in HCC tissues and cells. First, we collected 30 paired HCC and adjacent normal tissues, and detected *circ_0091579* expression, as shown in Figure 1A, a higher level of *circ_0091579* was exhibited in HCC tissues than that in normal group. Furthermore, *circ_0091579* level was also detected in HCC cell lines. Results showed that *circ_0091579* level was evidently up-regulated in SNU-387 and Huh7 cells compared with THLE-2 cells (Figure 1B). In addition, after the treatment of RNase R, *circ_0091579* was more resistant to RNase R than the linear form (*GPC3*) (Figure 1C and D). Besides, the cancer-specific circRNA database analyzed and described that *circ_0091579* was located in the *GPC3* gene and formed via head-to-tail splicing of *GPC3* exons 5–9 (Figure 1E). These results indicated

that the aberrant *circ_0091579* might be associated with HCC development.

Knockdown of *circ_0091579* Inhibits HCC Development in vitro

To study the role of *circ_0091579* in HCC development in vitro, *circ_0091579* abundance was knocked down in SNU-387 and Huh7 cells via transfection of si-*circ_0091579*-1 or si-*circ_0091579*-2 (Figure 2A). Meanwhile, *GPC3* expression was not changed (Figure 2B). The si-*circ_0091579* (si-*circ_0091579*-1) with the higher inhibitive efficacy on *circ_0091579* expression, and it was used for further experiments. The MTT assay showed that *circ_0091579* knockdown evidently suppressed the viability of SNU-387 and Huh7 cells (Figure 2C). Moreover, *circ_0091579* silence markedly reduced the abilities of migration and invasion in the two cell lines (Figure 2D). Additionally, the data of flow cytometry described that interference of *circ_0091579* evidently increased the cells at G0/G1 phase and decreased the cells at S phase (Figure 2E). Furthermore, the down-regulation of *circ_0091579* significantly repressed the colony formation ability (Figure 2F). Besides, inhibition of *circ_0091579* obviously induced SNU-387 and Huh7 cell apoptosis (Figure 2G). These data indicated that *circ_0091579* knockdown suppressed HCC development in SNU-387 and Huh7 cells.

miR-940 Knockdown Reverses the Function of *circ_0091579* Silence in HCC Development

By detecting the level of *circ_0091579* in nuclear and cytoplasmic fractions, we found that *circ_0091579* was mainly expressed in cytoplasm (Figure 3A), suggesting *circ_0091579* could serve as a ceRNA. The targets of *circ_0091579* were explored using CircInteractome, and the binding sequences of *circ_0091579* and *miR-940* are displayed in Figure 3B. To validate the interaction between *circ_0091579* and *miR-940*, we constructed the WT-*circ_0091579* and MUT-*circ_0091579* and transfected them into SNU-387 and Huh7 cells. The data of dual-luciferase reporter analysis displayed that *miR-940* overexpression decreased more than 70% luciferase activity of WT-*circ_0091579* in the two cell lines, while it did not alter the luciferase activity of MUT-*circ_0091579* (Figure 3C). Moreover, *miR-940* abundance was evidently reduced in HCC tissues and cell lines (SNU-387 and Huh7 cells) (Figure 3D and E). To analyze whether *miR-940* was

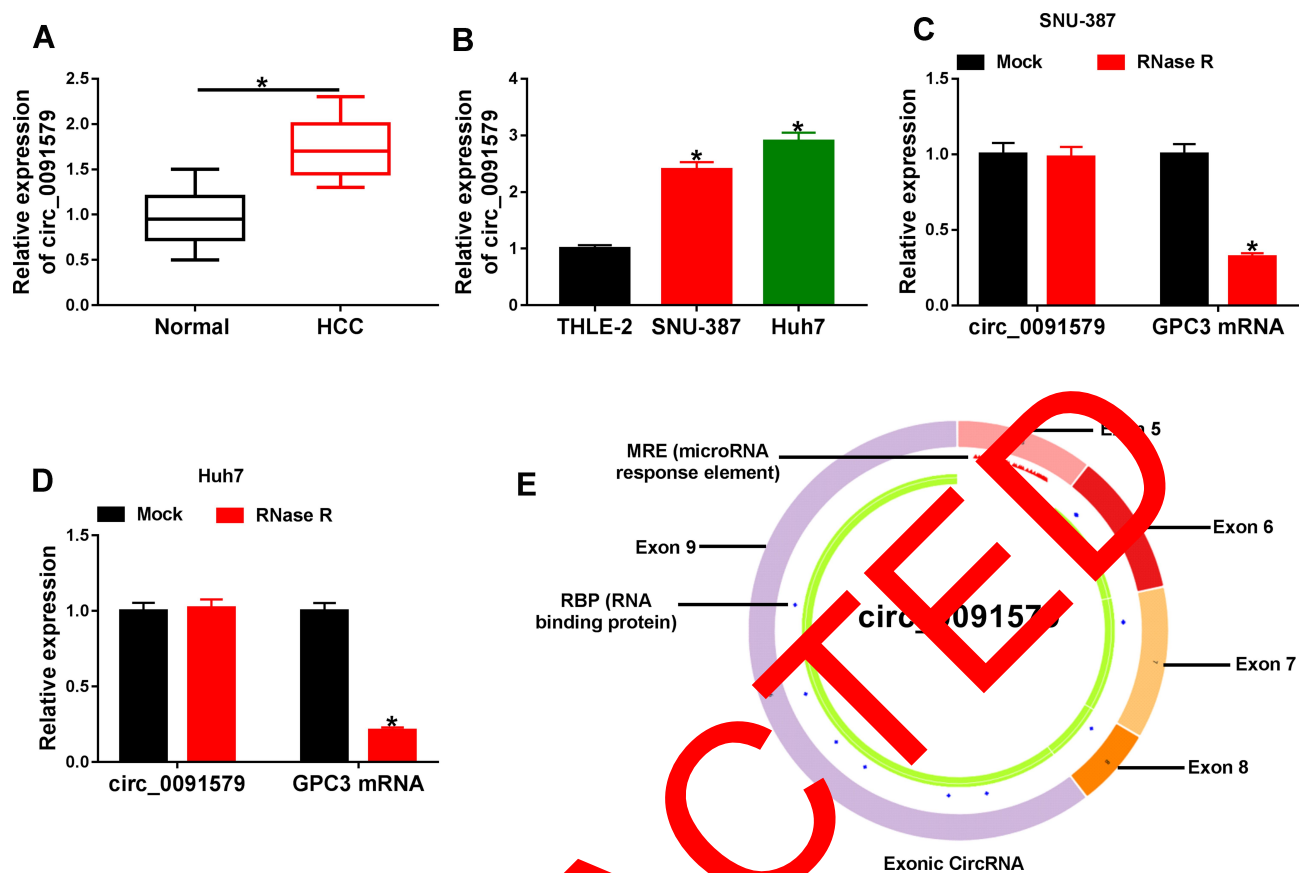


Figure 1 The expression of *circ_0091579* in HCC. (A) *circ_0091579* level was detected in HCC and adjacent normal tissues (n=30) via qRT-PCR. (B) *circ_0091579* expression was measured in HCC cell lines (SNU-387 and Huh7) and control cells (THLE-2) via qRT-PCR. (C and D) *circ_0091579* and *GPC3* mRNA levels were examined after treatment of RNase R in SNU-387 and Huh7 cells. (E) The structure of *circ_0091579* was analyzed via cancer-specific circRNA database. *P<0.05.

associated with *circ_0091579*-mediated HCC development, SNU-387 and Huh7 cells were transfected with mi-NC, si-*circ_0091579*, si-*circ_0091579* + *miR-940* inhibitor or inhibitor NC. The transfection efficacy of *miR-940* inhibitor is confirmed in Figure 3F. Furthermore, *miR-940* expression was increased via *circ_0091579* knockdown, which was weakened via transfection of *miR-940* inhibitor (Figure 3G). Besides, down-regulation of *miR-940* attenuated silence of *circ_0091579*-mediated suppression of cell viability, migration, invasion and colony formation, cell cycle arrest at G0/G1 phase, and promotion of apoptosis in SNU-387 and Huh7 cells (Figure 3H-L). These results indicated that *circ_0091579* regulated HCC development by mediating *miR-940*.

miR-940 Targets TACR1 to Suppress HCC Development in vitro

Next, the targets of *miR-940* were searched using TargetScan, and the binding sequences of *miR-940* and *TACR1* are displayed in Figure 4A. To identify the

relationship of *miR-940* and *TACR1*, we constructed the WT-*TACR1*-3'UTR and MUT-*TACR1*-3'UTR and transfected them into SNU-387 and Huh7 cells. The results showed that *miR-940* overexpression led to more than 67% reduction in luciferase activity of WT-*TACR1*-3'UTR, but it did not change the luciferase activity of MUT-*TACR1*-3'UTR (Figure 4B). Additionally, *TACR1* protein expression was significantly elevated in HCC tissues and cells (Figure 4C and D). To explore the function of *miR-940* and whether it required *TACR1*, SNU-387 and Huh7 cells were transfected with miRNA NC, *miR-940* mimic, *miR-940* mimic + pc-*TACR1* or pc-NC. The transfection efficacy of *miR-940* mimic and pc-*TACR1* was validated in Figure 4E and F. Moreover, *TACR1* protein expression was evidently declined via *miR-940* overexpression, which was restored by the introduction of pc-*TACR1* (Figure 4G). Besides, overexpression of *miR-940* evidently suppressed cell viability, migration, invasion and colony formation, induced cell cycle arrest at G0/G1 phase, and triggered cell apoptosis in SNU-387 and

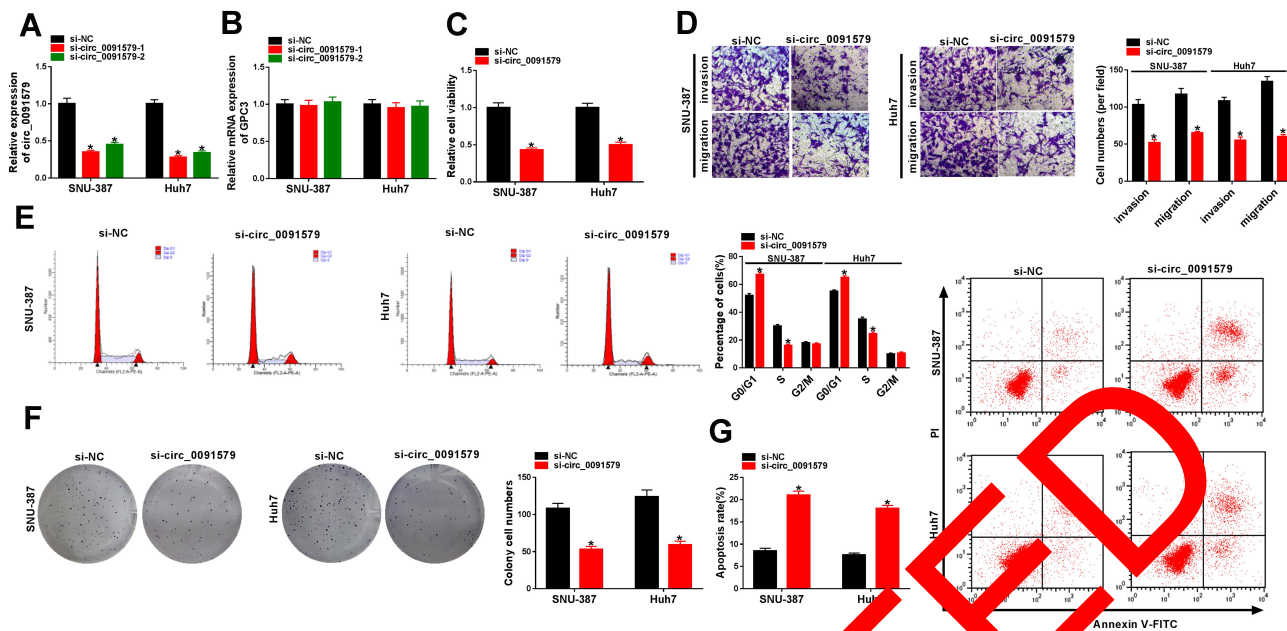


Figure 2 The influence of *circ_0091579* on HCC development in vitro. (A and B) The levels of *circ_0091579* and *GPC3* were measured in SNU-387 and Huh7 cells transfected with si-circ_0091579-1, si-circ_0091579-2 or si-NC. Cell viability (C), migration and invasion (D), cycle distribution (E), colony formation (F) and apoptosis (G) were detected in SNU-387 and Huh7 cells transfected with si-circ_0091579-1 (si-circ_0091579) or si-NC. *P<0.05.

Huh7 cells (Figure 4H–L). However, these events were mitigated by the restoration of *TACR1*. These data suggested that miR-940 regulated HCC development via targeting *TACR1*.

circ_0091579 Regulates *TACR1* Expression by miR-940

To test whether and how *circ_0091579* could mediate *TACR1*, the influence of *circ_0091579* on *TACR1* expression was investigated. As shown in Figure 5A and B, *TACR1* protein expression was evidently reduced via *circ_0091579* knockdown in SNU-387 and Huh7 cells, which was reversed via *TACR1* overexpression or miR-940 knockdown. These results indicated that *circ_0091579* could mediate *TACR1* by regulating miR-940.

circ_0091579 Knockdown Decreases Xenograft Tumor Growth

To explore the function of *circ_0091579* in HCC development in vivo, Huh7 cells with stable transfection of sh-circ_0091579 or sh-NC were applied to the establishment of xenograft model, and classified as sh-circ_0091579 or sh-NC group. After cell injection for 28 days, the volume and weight of the formed tumor were evidently reduced in sh-circ_0091579 group compared with sh-NC group (Figure 6A and B). Furthermore, the

abundances of *circ_0091579*, miR-940 and *TACR1* were detected in the formed tumor tissues. As displayed in Figure 6C, *circ_0091579* and *TACR1* levels were obviously declined in sh-circ_0091579 group, but miR-940 expression was enhanced. These data indicated that *circ_0091579* knockdown reduced HCC cell xenograft tumor growth.

Discussion

HCC is a major type of liver cancer worldwide.²⁶ The biological function of circRNA in HCC development is being a cutting edge.²⁷ Furthermore, the circRNA/miRNA/mRNA regulatory networks have key roles in the progression of HCC.²⁸ In this research, we tested the function of *circ_0091579* on HCC development and found the tumor-suppressive role of *circ_0091579* knockdown in HCC. Moreover, this study aimed to explore a novel ceRNA mechanism addressed via *circ_0091579*. Here we were the first to identify the ceRNA crosstalk of *circ_0091579/miR-940/TACR1* in HCC cells.

Zhang et al analyzed 20 dysregulated circRNAs using a circRNA microarray, and detected their expression in HCC via qRT-PCR.¹³ They found that *circ_0091579* was a highly expressed circRNA in HCC. However, the role and mechanism of *circ_0091579* in HCC are largely unclear. Niu et al suggested that *circ_0091579* could promote HCC development via increasing cell viability, colony formation and migration.²⁹

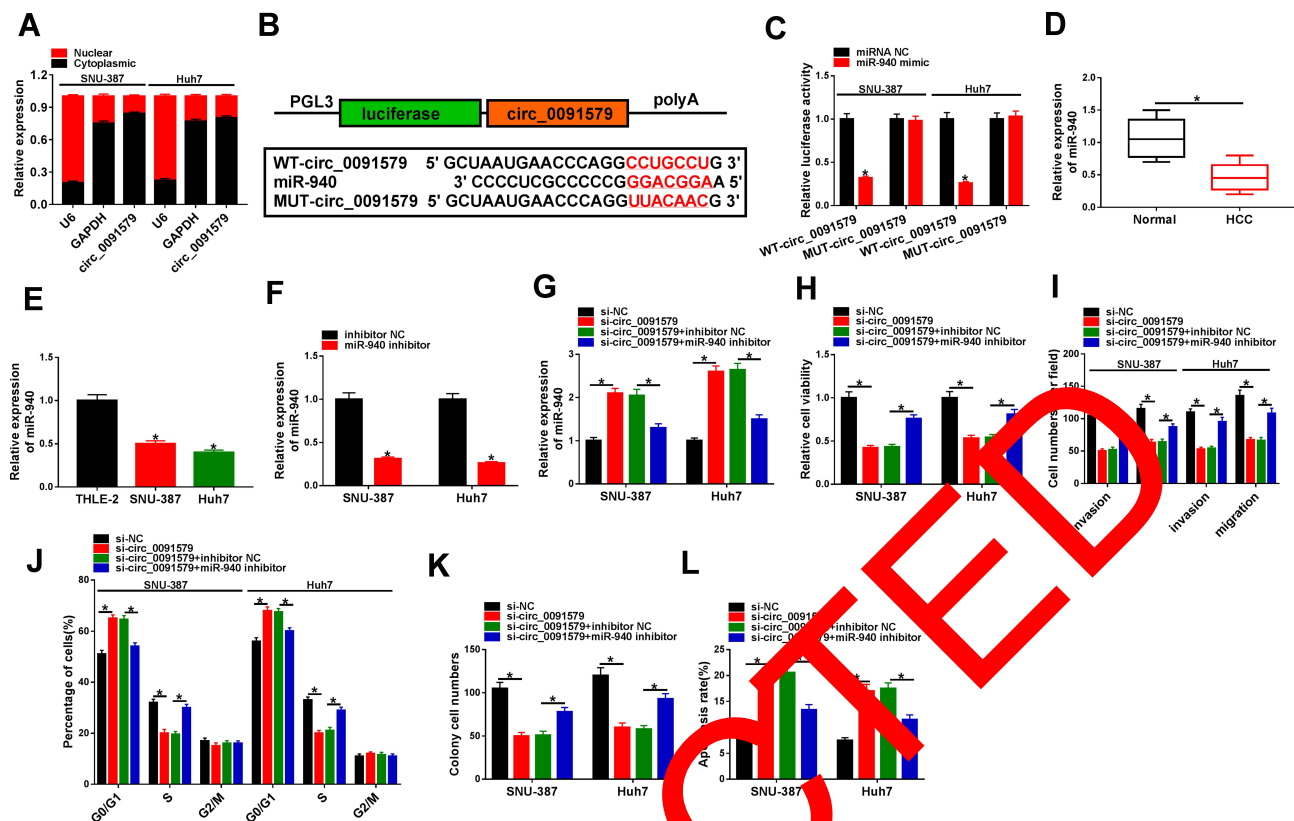


Figure 3 The effect of *miR-940* on *circ_0091579*-mediated HCC development in vitro. (A) *circ_0091579* expression in nuclear and cytoplasmic fractions. (B) The binding sites of *circ_0091579* and *miR-940*, and the construction of WT-*circ_0091579* and MUT-*circ_0091579*. (C) Luciferase activity was detected in SNU-387 and Huh7 cells transfected with WT-*circ_0091579* or MUT-*circ_0091579* and *miR-940* mimic or miRNA NC. (D) *miR-940* expression was measured in HCC and normal tissues (n=30). (E) *miR-940* level was detected in SNU-387, Huh7 and THLE-2 cells. (F) *miR-940* expression was examined in SNU-387 and Huh7 cells with transfection of *miR-940* inhibitor or inhibitor NC. *miR-940* level (G), cell viability (H), migration and invasion (I), cell cycle distribution (J), colony formation (K) and apoptosis (L) were examined in SNU-387 and Huh7 cells transfected with si-NC, si-*circ_0091579*, si-*circ_0091579*+*miR-940* inhibitor or inhibitor NC. **P*<0.05.

Similarly, we also confirmed these events. Moreover, we further validated that *circ_0091579* knockdown could regulate HCC cell invasion and induce cell cycle arrest at G0/G1 phase and cell apoptosis. Collectively, our study indicated the oncogenic role of *circ_0091579* in HCC development in vitro.

The circRNA-mediated ceRNA network is the main mechanism for ceRNA in HCC development.³⁰ A previous study indicated that *circ_0091579* could sponge *miR-940* in liver cancer.²⁹ This study confirmed that *miR-940* was targeted via *circ_0091579*. Here we found that *miR-940* level was reduced in HCC tissues and cells, which was also in agreement with the previous study.³¹ The former evidences suggested that *miR-940* could inhibit HCC cell growth, migration and invasion.^{16,17} Similarly, we also found that *miR-940* overexpression repressed HCC development by decreasing cell viability, colony formation, migration and invasion, inducing cycle arrest at G0/G1 phase, and promoting apoptosis, which was also consistent with that in many other cancers, such as tongue squamous cell carcinoma, glioma and esophageal squamous cell carcinoma.^{32–}

³⁴ However, it was opposite to that in endometrial carcinoma.³⁵ We hypothesized it might be caused by the alteration of tumor microenvironment. Our study indicated the anti-cancer role of *miR-940* in HCC development. Furthermore, we found that *circ_0091579* could mediate HCC development via regulating *miR-940*.

Next, we validated the interaction between *miR-940* and *TACR1*. A previous study suggested that *TACR1* functioned as an oncogene in HCC development.²⁰ In our study, *TACR1* expression was enhanced in HCC, indicating the potential carcinogenic role of *TACR1* in HCC. Moreover, we identified the oncogenic role of *TACR1* in HCC by reversing the anti-cancer function of *miR-940*, which was also similar to that in neuroblastoma.¹⁹ Besides, our results validated that *circ_0091579* could regulate *TACR1* expression via competitively binding with *miR-940*, implying that *circ_0091579* might target *TACR1* by mediating *miR-940* to be involved in HCC development in vitro. In xenograft model with nude mice as hosts, the tumors are formed via the injection of cancer cells, which could be used to assess the pathogenesis

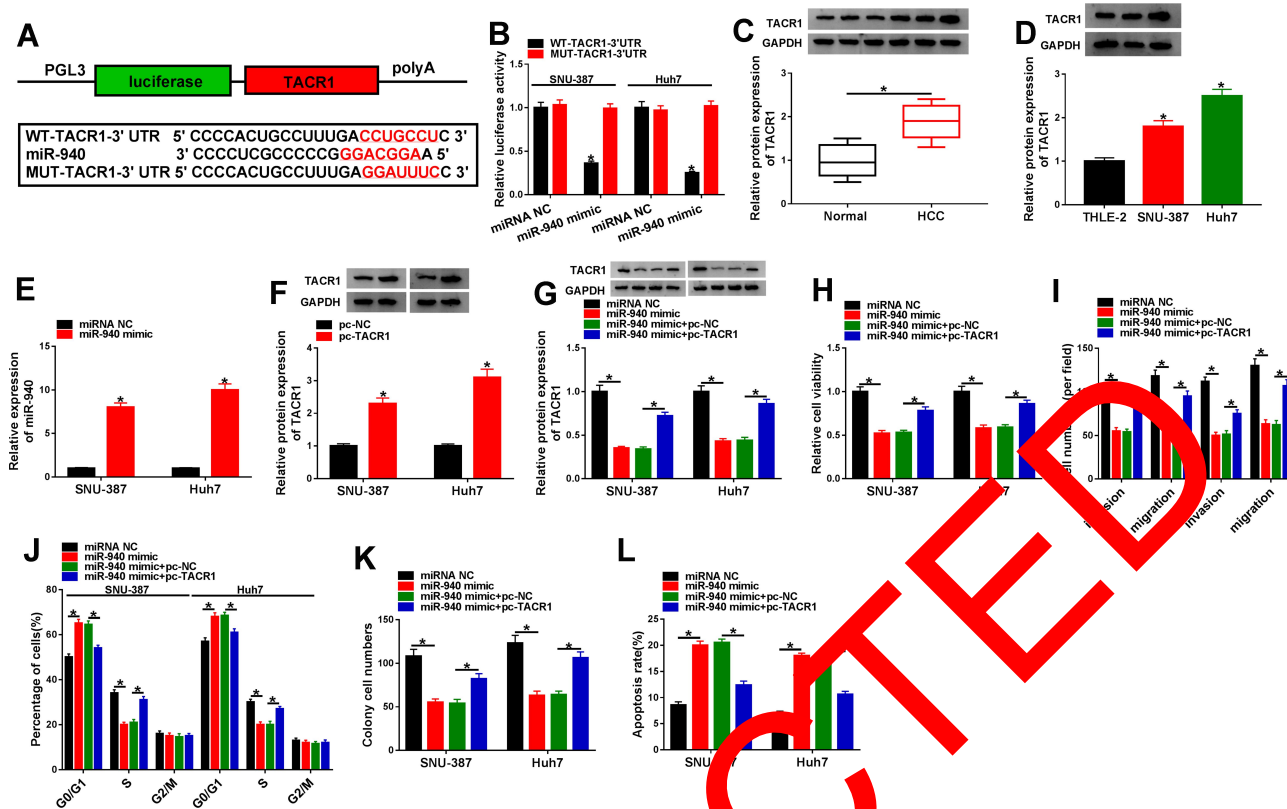


Figure 4 The effect of *miR-940* and *TACR1* on HCC development in vitro. (A) The binding sequences of *miR-940* and *TACR1*, and the construction of WT-*TACR1*-3'UTR and MUT-*TACR1*-3'UTR. (B) Luciferase activity was examined in SNU-387 and Huh7 cells transfected with WT-*TACR1*-3'UTR or MUT-*TACR1*-3'UTR and *miR-940* mimic or miRNA NC. (C) *TACR1* protein level was measured in HCC and normal tissues. (D) *TACR1* protein level was examined in SNU-387, Huh7 and THLE-2 cells. (E) *miR-940* abundance was examined in SNU-387 and Huh7 cells with transfection of *miR-940* mimic or miRNA NC. (F) *TACR1* protein expression was measured in SNU-387 and Huh7 cells with transfection of pc-*TACR1* or pc-NC. *TACR1* protein level (G), cell viability (H), migration and invasion (I), cycle distribution (J), colony formation (K) and apoptosis (L) were determined in SNU-387 and Huh7 cells with transfection of miRNA NC, *miR-940* mimic, *miR-940* mimic + pc-*TACR1* or pc-NC. **P*<0.05.

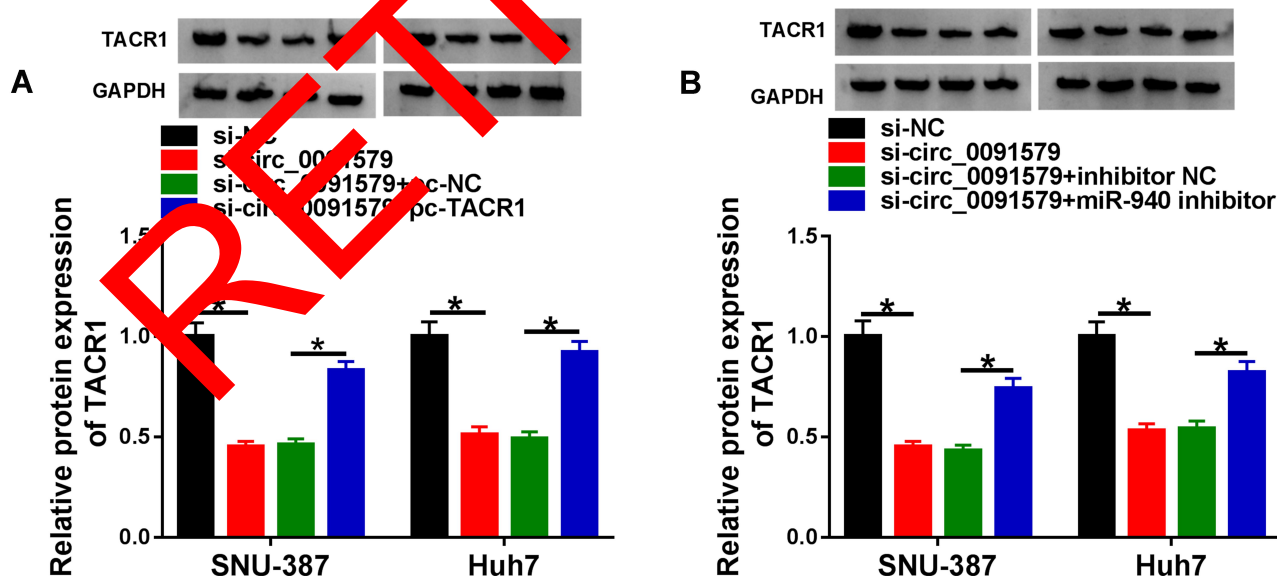


Figure 5 The effect of *circ_0091579* on *TACR1* expression. (A) *TACR1* protein expression was measured in SNU-387 and Huh7 cells transfected with si-NC, si-*circ_0091579*, si-*circ_0091579* + pc-*TACR1* or pc-NC. (B) *TACR1* protein level was detected in SNU-387 and Huh7 cells transfected with si-NC, si-*circ_0091579*, si-*circ_0091579* + *miR-940* inhibitor or inhibitor NC. **P*<0.05.

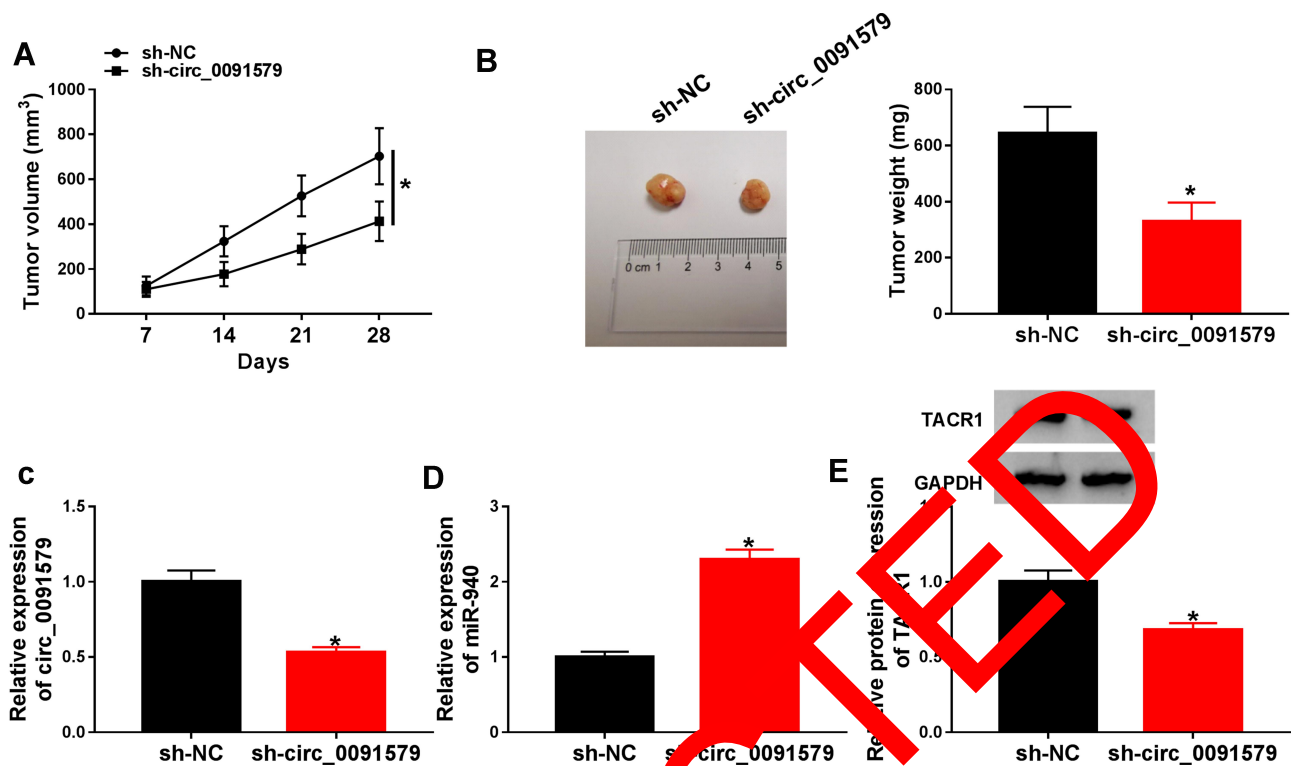


Figure 6 The effect of *circ_0091579* on xenograft tumor growth. (A and B) Tumor volume and weight were examined in xenograft tumor that was formed by Huh7 cells with transfection of sh-*circ_0091579* or sh-NC. (C–E) *circ_0091579*, *miR-940* and *TACR1* levels were detected in xenograft tumor that was formed by Huh7 cells with transfection of sh-*circ_0091579* or sh-NC. * $P < 0.05$.

of HCC in vivo.³⁶ To further explore the anti-cancer role of *circ_0091579* in HCC in vivo, we established the murine xenograft model by injecting Huh7 cells and confirmed that knockdown of *circ_0091579* could decrease the tumor growth, which was associated with *miR-940/TACR1* axis.

Conclusion

In conclusion, our study validated that *circ_0091579* knockdown repressed HCC development in vitro and in vivo, possibly via mediating *miR-940/TACR1* axis in a ceRNA-based mechanism. This research indicates a new mechanism for understanding the pathogenesis of HCC.

Acknowledgments

The authors would like to thank the participants in this study.

Funding

There is no funding to report.

Disclosure

The authors declare that they have no conflicts of interest in this work.

References

- Forner A, Reig M, Bruix J. Hepatocellular carcinoma. *Lancet*. 2018;391(10127):1301–1314. doi:10.1016/S0140-6736(18)30010-2
- Grandhi MS, Kim AK, Ronnekleiv-Kelly SM, et al. Hepatocellular carcinoma: from diagnosis to treatment. *Surg Oncol*. 2016;25:74–85. doi:10.1016/j.suronc.2016.03.002
- Dutta R, Mahato RI. Recent advances in hepatocellular carcinoma therapy. *Pharmacol Ther*. 2017;173:106–117. doi:10.1016/j.pharmthera.2017.02.010
- Yin Y, Long J, He Q, et al. Emerging roles of circRNA in formation and progression of cancer. *J Cancer*. 2019;10:5015–5021. doi:10.7150/jca.30828
- Wang M, Yu F, Li P. Circular RNAs: characteristics, function and clinical significance in hepatocellular carcinoma. *Cancers (Basel)*. 2018;10:258. doi:10.3390/cancers10080258
- Xiong DD, Dang YW, Lin P, et al. A circRNA-miRNA-mRNA network identification for exploring underlying pathogenesis and therapy strategy of hepatocellular carcinoma. *J Transl Med*. 2018;16:220. doi:10.1186/s12967-018-1593-5
- Yao Z, Xu R, Yuan L, et al. Circ_0001955 facilitates hepatocellular carcinoma (HCC) tumorigenesis by sponging miR-516a-5p to release TRAF6 and MAPK11. *Cell Death Dis*. 2019;10:945. doi:10.1038/s41419-019-2176-y
- Li Z, Liu Y, Yan J, et al. Circular RNA hsa_circ_0056836 functions as an oncogenic gene in hepatocellular carcinoma through modulating miR-766-3p/FOSL2 axis. *Aging (Albany NY)*. 2020;12:2485–2497. doi:10.18632/aging.102756
- Pu J, Wang J, Li W, et al. hsa_circ_0000092 promotes hepatocellular carcinoma progression through up-regulating HN1 expression by binding to microRNA-338-3p. *J Cell Mol Med*. 2020. doi:10.1111/jcmm.15010

10. Liu Z, Yu Y, Huang Z, et al. CircRNA-5692 inhibits the progression of hepatocellular carcinoma by sponging miR-328-5p to enhance DAB2IP expression. *Cell Death Dis.* 2019;10(12):900. doi:10.1038/s41419-019-2089-9
11. Su X, Su J, He H, et al. Hsa_circ_0070269 inhibits hepatocellular carcinoma progression through modulating miR-182/NPTX1 axis. *Biomed Pharmacother.* 2019;120:109497. doi:10.1016/j.biopha.2019.109497
12. Chen H, Liu S, Li M, et al. circ_0003418 inhibits tumorigenesis and cisplatin chemoresistance through Wnt/beta-catenin pathway in hepatocellular carcinoma. *Onco Targets Ther.* 2019;12:9539–9549. doi:10.2147/OTT.S229507
13. Zhang C, Zhang C, Lin J, et al. Circular RNA Hsa_Circ_0091579 serves as a diagnostic and prognostic marker for hepatocellular carcinoma. *Cell Physiol Biochem.* 2018;51:290–300. doi:10.1159/000495230
14. Mahgoub A, Steer CJ. MicroRNAs in the evaluation and potential treatment of liver diseases. *J Clin Med.* 2016;5:52. doi:10.3390/jcm5050052
15. Anwar SL, Lehmann U. MicroRNAs: emerging novel clinical biomarkers for hepatocellular carcinomas. *J Clin Med.* 2015;4:1631–1650. doi:10.3390/jcm4081631
16. Yuan B, Liang Y, Wang D, et al. MiR-940 inhibits hepatocellular carcinoma growth and correlates with prognosis of hepatocellular carcinoma patients. *Cancer Sci.* 2015;106:819–824. doi:10.1111/cas.12688
17. Ding D, Zhang Y, Yang R, et al. miR-940 suppresses tumor cell invasion and migration via regulation of CXCR2 in hepatocellular carcinoma. *Biomed Res Int.* 2016;2016:7618342. doi:10.1155/2016/7618342
18. Xu H, Sun Y, Ma Z, et al. LOC134466 methylation promotes oncogenesis of endometrial carcinoma through LOC134466/hsa-miR-196a-5p/TAC1 axis. *Aging (Albany NY).* 2018;10:3353–3364. doi:10.18632/aging.101644
19. Pan J, Zhang D, Zhang J, et al. LncRNA RMRP silence curbs neonatal neuroblastoma progression by regulating miR-206/tachykinin-1 receptor axis via inactivating extracellular signal-regulated kinases. *Cancer Biol Ther.* 2019;20:659–665. doi:10.1080/15384047.2018.1550568
20. Hongfeng Z, Andong J, Liwen S, et al. LncRNA RMRP knockdown suppress hepatocellular carcinoma biological activities by regulation miRNA-206/TACR1. *J Cell Biochem.* 2020;121:1699–1702. doi:10.1002/jcb.29404
21. Dudekula DB, Panda AC, Gramatikakis I, et al. CircInteractome: a web tool for exploring circular RNAs and their interacting proteins and microRNAs. *RNA Biol.* 2016;13:34–42. doi:10.1080/15476286.2015.1128065
22. Riffo-Campos AL, Riquelme J, Brebièveville P. Tools for sequence-based miRNA target prediction: what to choose? *Int J Mol Sci.* 2016;17:1987. doi:10.3390/ijms17121987
23. Chomczynski P, Sacchi N. The single-step method of RNA isolation by acid guanidinium thiocyanate-phenol-chloroform extraction: twenty-something years on. *Nat Protoc.* 2006;1:581–585. doi:10.1038/nprot.2006.83
24. Livak KJ, Schmittgen TD. Analysis of relative gene expression data using real-time quantitative PCR and the 2(-Delta Delta C(T)) method. *Methods.* 2001;25:402–408. doi:10.1006/meth.2001.1262
25. Xia S, Feng J, Chen K, et al. CSCD: a database for cancer-specific circular RNAs. *Nucleic Acids Res.* 2018;46:D925–D929. doi:10.1093/nar/gkx863
26. Villanueva A. Hepatocellular Carcinoma. *N Engl J Med.* 2019;380:1450–1462. doi:10.1056/NEJMra1713263
27. Qiu L, Xu H, Ji M, et al. Circular RNAs in hepatocellular carcinoma: biomarkers, functions and mechanisms. *Life Sci.* 2019;231:116660. doi:10.1016/j.lfs.2019.116660
28. Sun X, Ge X, Xu Z, et al. Identification of circular RNA-microRNA-messenger RNA regulatory network in hepatocellular carcinoma by integrated analysis. *J Gastroenterol Hepatol.* 2020;35:157–164. doi:10.1111/jgh.14762
29. Niu WY, Chen L, Zhang P, et al. Circ_0091579 promotes proliferative ability and metastasis of liver cancer cells by regulating microRNA-490-3p. *Eur Rev Med Pharmacol Sci.* 2019;23:10264–10270. doi:10.26155/eurev.201912.19664
30. Wu J, Liu S, Liang Y, et al. Bioinformatic analysis of circular RNA-associated miRNA network associated with hepatocellular carcinoma. *Biomed Res Int.* 2019;2019:8308694. doi:10.1155/2019/8308694
31. Li Y, Zhao Z, Luo J, et al. miR-139-5p, miR-940 and miR-193a-5p inhibit the growth of hepatocellular carcinoma by targeting SPOCK1. *J Cell Mol Med.* 2019;23:2475–2488. doi:10.1111/jcmm.14121
32. Li T, Zhao Z, Wang Z, et al. MiR-940 inhibits migration and invasion of tongue squamous cell carcinoma via regulating CXCR2/NF-kappaB system-mediated epithelial-mesenchymal transition. *Munchn Schmiedebergs Arch Pharmacol.* 2019;392:1359–1369. doi:10.1007/s00210-019-01671-w
33. Luo H, Xu R, Chen B, et al. MicroRNA-940 inhibits glioma cells proliferation and cell cycle progression by targeting CKS1. *Am J Transl Res.* 2019;11:4851–4865.
34. Wang H, Song T, Qiao Y, et al. miR-940 inhibits cell proliferation and promotes apoptosis in esophageal squamous cell carcinoma cells and is associated with post-operative prognosis. *Exp Ther Med.* 2020;19:833–840. doi:10.3892/etm.2019.8279
35. Zhou Z, Xu Y, Wang L, et al. miR-940 potentially promotes proliferation and metastasis of endometrial carcinoma through regulation of MRV11. *Biosci Rep.* 2019;39:BSR20190077. doi:10.1042/bsr20190077
36. Heindryckx F, Colle I, Van Vlierberghe H. Experimental mouse models for hepatocellular carcinoma research. *Int J Exp Pathol.* 2009;90:367–386. doi:10.1111/j.1365-2613.2009.00656.x

Cancer Management and Research

Dovepress

Publish your work in this journal

Cancer Management and Research is an international, peer-reviewed open access journal focusing on cancer research and the optimal use of preventative and integrated treatment interventions to achieve improved outcomes, enhanced survival and quality of life for the cancer patient.

The manuscript management system is completely online and includes a very quick and fair peer-review system, which is all easy to use. Visit <http://www.dovepress.com/testimonials.php> to read real quotes from published authors.

Submit your manuscript here: <https://www.dovepress.com/cancer-management-and-research-journal>